On the Wind Power Input to the Ocean General Circulation

XIAOMING ZHAI

Atmospheric, Oceanic and Planetary Physics, University of Oxford, Oxford, United Kingdom

HELEN L. JOHNSON

Department of Earth Sciences, University of Oxford, Oxford, United Kingdom

DAVID P. MARSHALL

Atmospheric, Oceanic and Planetary Physics, University of Oxford, Oxford, United Kingdom

CARL WUNSCH

Department of Earth, Atmospheric and Planetary Sciences, Massachusetts Institute of Technology, Cambridge, Massachusetts

(Manuscript received 12 January 2012, in final form 3 May 2012)

ABSTRACT

The wind power input to the ocean general circulation is usually calculated from the time-averaged wind products. Here, this wind power input is reexamined using available observations, focusing on the role of the synoptically varying wind. Power input to the ocean general circulation is found to increase by over 70% when 6-hourly winds are used instead of monthly winds. Much of the increase occurs in the storm-track regions of the Southern Ocean, Gulf Stream, and Kuroshio Extension. This result holds irrespective of whether the ocean surface velocity is accounted for in the wind stress calculation. Depending on the fate of the high-frequency wind power input, the power input to the ocean general circulation relevant to deep-ocean mixing may be less than previously thought. This study emphasizes the difficulty of choosing appropriate forcing for ocean-only models.

1. Introduction

The mechanical energy input to the ocean by atmospheric winds is a major energy source for driving the large-scale ocean circulation and maintaining the abyssal stratification (e.g., Ferrari and Wunsch 2009). Power input to the ocean can be regarded as a transfer of atmospheric kinetic energy into the ocean, reflected in the wind stress bulk formula, which depends quadratically on the wind,

$$\boldsymbol{\tau} = \rho_a c_d |\mathbf{U}_{10} - \mathbf{u}_o|(\mathbf{U}_{10} - \mathbf{u}_o), \tag{1}$$

where $\boldsymbol{\tau}$ is the surface wind stress; ρ_a is the density of air at sea level; c_d is the drag coefficient; $\mathbf{u}_o$ is the ocean surface velocity; and $\mathbf{U}_{10}$ is the wind velocity, or simply wind, at 10 m above the sea surface. Note that the drag coefficient itself varies with wind speed, as well as the air–sea temperature difference, but these variations are not considered here and we set c_d = constant. One consequence of the quadratic dependence of the wind stress on the wind itself is that the high-frequency wind does not simply average out but contributes to the time-averaged wind stress (e.g., Thompson et al. 1983). For example, the monthly-mean wind stress is not to be confused with the stress associated with the monthly-mean wind. The wind power input to the large-scale geostrophic ocean circulation has sometimes been suggested to be dominated by the time-mean wind. Although this may be true in regions where there is little wind variability, it breaks down in regions where the synoptic wind dominates: for example, the storm-track regions. Because the storm-track regions are also regions where the wind power input is most significant (e.g., Wunsch 1998; von Storch et al. 2007; Hughes and Wilson 2008;

Corresponding author address: Xiaoming Zhai, School of Environmental Sciences, University of East Anglia, Norwich NR4 7TJ, United Kingdom.
E-mail: xiaoming.zhai@uea.ac.uk

DOI: 10.1175/JPO-D-12-09.1

Scott and Xu 2009), the synoptic wind input is likely a nonnegligible contribution to the global total.

Note that the wind power input to the large-scale geostrophic circulation, which is the focus of the present study, is only part of the total wind power input to the ocean. However, the wind power input to surface waves and surface ageostrophic currents, although of much larger magnitude, tends to be dissipated within the surface layer and is therefore not available to the deep ocean (e.g., von Storch et al. 2007; Zhai et al. 2009).

Over most of the ocean the speed of ocean surface currents is at least one order of magnitude smaller than that of the 10-m wind, and the wind stress is thus often computed using the 10-m wind alone, neglecting the contribution from the surface ocean currents. Recently, a few studies (e.g., Duhaut and Straub 2006; Zhai and Greatbatch 2007; Hughes and Wilson 2008; Scott and Xu 2009) have found a positive bias in calculations of wind power input (about 20%–30%) if the relative air–sea velocities are not accounted for in the stress calculation. Not accounting for ocean surface velocity in the stress calculation is hereafter referred to as the ''resting ocean approximation.''

Attempts to interpret physically the cause of the positive bias have, in the past, emphasized the smaller spatial scales of ocean currents and the vortex structure of ocean eddies (Zhai and Greatbatch 2007; Hughes and Wilson 2008), schematically illustrated in Fig. 1a. When the wind blows over the eddy shown, the stress is smaller on the northern side because wind and current are aligned and larger on the southern side where they oppose each other. The net effect, when integrated spatially, takes energy out of the eddy: that is, the wind mechanically damps the eddy.

An overlooked aspect, however, is that the atmospheric wind tends to vary on faster time scales than do surface geostrophic currents. At a fixed location in space, the synoptically varying wind tends to damp the underlying ocean currents, regardless of their spatial structure. This situation is illustrated schematically in Fig. 1b for the case of an oscillating wind blowing over a steady current. When the wind is aligned with the current, the stress is smaller than in the motionless ocean case and hence the wind does less positive work. When the wind opposes the current, the stress is larger and hence does more negative work. Integrated over time, the energy is removed from the current, damping the flow. Both damping effects illustrated in Fig. 1 are termed here the ''wind mechanical damping effect.''

In this paper, the wind power input to the ocean general circulation is reexamined using available observations. Of particular interest is the role of the synoptic wind in supplying energy to the ocean general circulation and in taking energy out of the ocean when the ocean surface velocity is taken into account in the wind stress calculation.

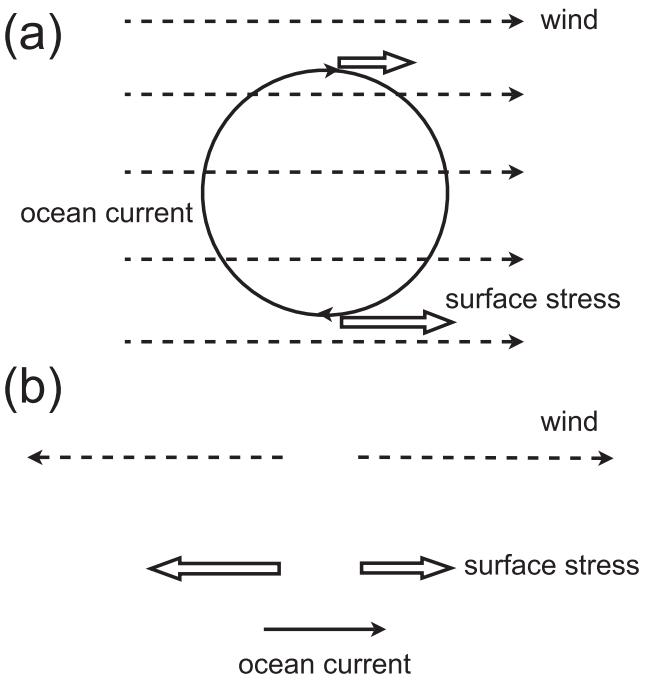

FIG. 1. Schematic illustrating the mechanical damping effect by the wind. The dashed line denotes the wind; the solid line denotes the surface ocean current; and the open arrow denotes the surface stress, which depends on the relative motion between the air and the surface ocean. (a) The wind blows over an eddy, where the stress is smaller on the northern side because wind and current are aligned and larger on the southern side because they oppose each other. The net effect, when integrated spatially, takes energy out of the eddy: that is, the wind mechanically damps the eddy. (b) An oscillating wind blows over a steady current. When the wind is aligned with the current, the stress is smaller than in the motionless ocean case and hence the wind does less positive work. When the wind opposes the current, the stress is larger and hence does more negative work. Integrated over time, the energy is removed from the current, damping the flow. Both damping effects illustrated in the schematic are termed the wind mechanical damping effect.

2. Theory

a. With the resting ocean approximation

First consider the wind stress equation in (1) with the resting ocean approximation (i.e., setting $\mathbf{u}_o = 0$) and focus on the effect relating to the part of the stress aligned with the 10-m wind. For simplicity, it is assumed that c_d is constant and the mean wind blows eastward. The derivation here serves a pedagogical purpose, but the results are general and easily extended to two dimensions. Wind variability is introduced by increasing and decreasing the wind speed by a factor a at two consecutive times. The stress at these times is then

$$\tau_{1,2} = \rho_a c_d |U_{10} \pm \alpha U_{10}|(U_{10} \pm \alpha U_{10}), \quad (2)$$

and the time-averaged stress is

$$\overline{\tau} = \frac{\tau_1 + \tau_2}{2} = \begin{cases} (1+\alpha^2)\rho_a c_d U_{10}^2 = (1+\alpha^2)\tau \geq \tau & \text{for} \quad \alpha \leq 1, \\ 2\alpha\rho_a c_d U_{10}^2 = 2\alpha\tau > \tau & \text{for} \quad \alpha > 1, \end{cases} \quad (3)$$

from the triangle inequality $a^2 + b^2 \geq (a+b)^2/2$. Therefore, even though the time-varying wind has the same time-mean wind speed as the constant wind, the time-averaged stress associated with the time-varying wind under the resting ocean approximation can be much larger than that associated with the constant wind. This result is consistent with the notion that the work done by the wind on the ocean is a transfer of atmospheric kinetic energy into the ocean, which includes kinetic energy associated with both the mean and synoptic winds.

Alternatively, assume

$$U_{10} = \overline{U}_{10}(1 + \alpha z_t), \quad (4)$$

where $\overline{U}_{10}$ is the time-mean 10-m wind and z_t is the stochastic component of U_{10} with zero mean and unit variance [i.e., $z_t \sim \mathcal{N}(0, 1)$]. The time-averaged wind stress is (see appendix A)

$$\overline{\tau} = \rho_a c_d \overline{U}_{10}^2 \left[(1+\alpha^2)\,\mathrm{erf}\left(\frac{1}{\sqrt{2}\alpha}\right) + \sqrt{\frac{2}{\pi}}\alpha e^{-(1/2\alpha^2)} \right] \approx \begin{cases} (1+\alpha^2)\tau & \text{for} \quad \alpha \ll 1, \\ 1.6\alpha\tau & \text{for} \quad \alpha \gg 1, \end{cases} \quad (5)$$

consistent with (3), except that the factor 2 is replaced by 1.6 in the final expression. The general variation of $\overline{\tau}$ with α is plotted in Fig. 2.

b. Without the resting ocean approximation

Retain now the ocean surface velocity dependence in the wind stress formula. For simplicity, u_o is assumed to be sufficiently small such that $U_{10} - u_o$ is again positive. The difference between the wind stress without the resting ocean approximation τ_{DS} and that with the resting ocean approximation τ is given by

$$\Delta\tau = \tau_{\mathrm{DS}} - \tau = -2\rho_a c_d U_{10} u_o + \rho_a c_d u_o^2. \quad (6)$$

Again, after increasing and decreasing the wind speed by a factor α at two consecutive times,

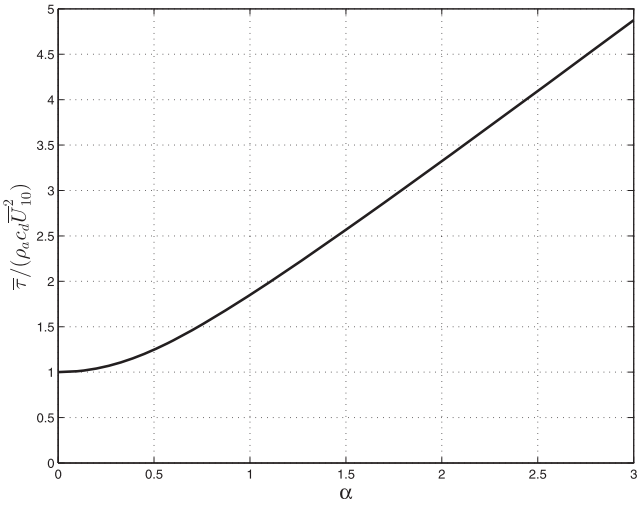

FIG. 2. The time-averaged wind stress $[\overline{\tau}/(\rho_a c_d \overline{U}_{10}^2)]$ as a function of the stochastic wind variability (measured by α). See Eq. (5) for the actual function.

$$\tau_{\mathrm{DS}1,2} = \rho_a c_d |U_{10} \pm \alpha U_{10} - u_o|(U_{10} \pm \alpha U_{10} - u_o),$$

the time-averaged stress is

$$\overline{\tau}_{\mathrm{DS}} = \frac{\tau_{\mathrm{DS}1} + \tau_{\mathrm{DS}2}}{2} = \begin{cases} \rho_a c_d [(1+\alpha^2)U_{10}^2 - 2U_{10}u_o + u_o^2] & \text{for} \quad \alpha \leq 1, \\ 2\alpha\rho_a c_d U_{10}(U_{10} - u_o) & \text{for} \quad \alpha > 1. \end{cases} \quad (7)$$

With u_o,

$$\Delta\overline{\tau}_{\mathrm{DS}} = \overline{\tau}_{\mathrm{DS}} - \overline{\tau} = \begin{cases} -2\rho_a c_d U_{10} u_o + \rho_a c_d u_o^2 = \Delta\tau & \text{for} \quad \alpha \leq 1, \\ -2\alpha\rho_a c_d U_{10} u_o < \Delta\tau & \text{for} \quad \alpha > 1. \end{cases} \quad (8)$$

Thus, the mechanical damping effect by the time-varying wind is greater than that by the constant wind when the time-varying wind changes direction: that is, $\alpha > 1$. These results are consistent with the finding of Duhaut and Straub (2006): that is, without the resting ocean approximation, the mechanical damping effect by the wind depends linearly on the wind speed.

The analysis can be repeated with both stochastic wind variability and stochastic ocean current variability, assuming both the mean and stochastic ocean current speeds are an order of magnitude smaller than the mean and stochastic wind speeds. As detailed in appendix A, it is found that

$$\Delta\overline{\tau}_{\mathrm{DS}} \approx \begin{cases} -2\rho_a c_d U_{10} u_o & \text{for} \quad \alpha \ll 1, \\ -1.6\alpha\rho_a c_d U_{10} u_o & \text{for} \quad \alpha \gg 1, \end{cases} \quad (9)$$

consistent with (8) in the limit $|u_o| \ll |U_{10}|$. Note that these results are unaffected, at leading order, by stochastic variations in ocean current speeds.

In the next section, the above ideas are tested using available observations.

3. Data

Following Hughes and Wilson (2008), the absolute sea surface height (SSH) for the period from January 1995 to December 2008 is obtained by combining the ocean mean dynamic height from the Maximenko and Niiler (2005) product and the SSH anomaly product compiled by the Collecte Localisation Satellites (CLS) Space Oceanographic Division of Toulouse, France. The SSH anomaly values result from merging the Ocean Topography Experiment (TOPEX)/Poseidon and *European Remote Sensing Satellite-1* (*ERS-1*)/*ERS-2* along-track SSH measurements for a temporal gridding of 7 days on a 1/3° Mercator grid (Le Traon et al. 1998). The Maximenko and Niiler (2005) product, which integrates information from surface drifters, satellite altimetry, surface winds, and the Gravity Recovery and Climate Experiment (GRACE) gravity mission for the period from 1992 to 2002, is interpolated from a 1/2° latitude–longitude grid to the same grid as the SSH anomalies. Surface currents $\mathbf{u}_g$ are then computed through geostrophy from the absolute SSH with temporal resolution of 7 days. Readers are referred to Hughes and Wilson (2008) and Scott and Xu (2009) for a detailed discussion of errors associated with each product.

The 6-hourly, daily, and monthly 10-m wind fields are taken from the National Centers for Environmental Prediction (NCEP) reanalysis product (Kalnay et al. 1996) and interpolated to the same grid as $\mathbf{u}_g$. Surface wind stress is then computed from 10- m wind using the Large et al. (1994) formula for the drag coefficient and $\rho_a = 1.223$ kg m^{-3}. There are subtle issues associated with the drag coefficient (e.g., whether the same drag coefficient should be used for both the resting and nonresting ocean cases), but these issues are not considered in the present study. The wind power input to the ocean general circulation is finally computed as $\overline{\boldsymbol{\tau} \cdot \mathbf{u}_g}$, where the overbar denotes the 14-yr time average. For comparison, power input is also computed using the monthly-mean NCEP wind stress taken directly from the reanalysis product. Note that the monthly-mean NCEP wind stress is a monthly average of the instantaneous surface wind stress at every 20-min NCEP model time step. Determining the accuracy of the 20-min interval NCEP stress calculation is beyond our present scope; it is here treated as a plausible reference value only.

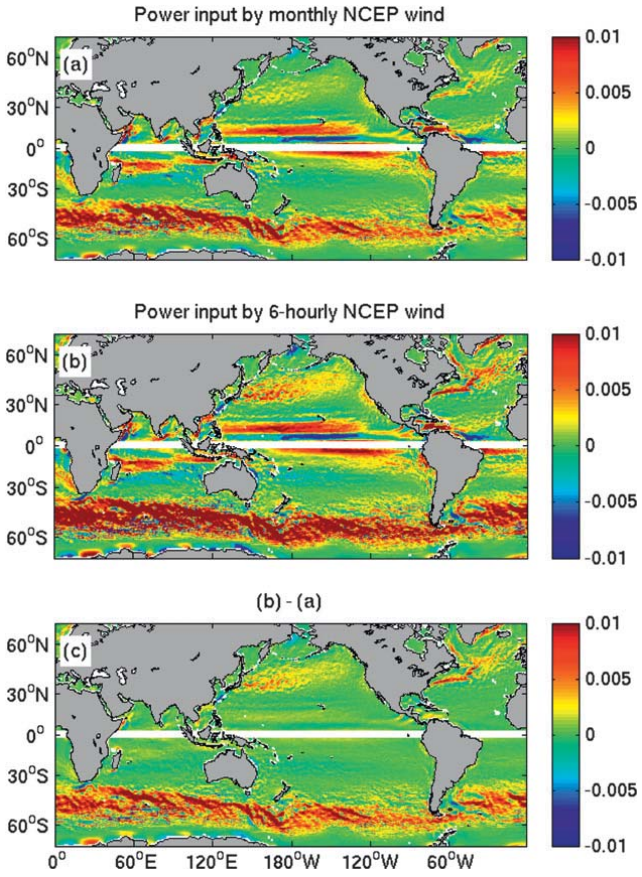

FIG. 3. Power input (W m^{-2}) by (a) the monthly NCEP wind and (b) the 6-hourly NCEP wind with the resting ocean approximation. (c) Shown is (b) minus (a). The color bar is saturated. The maximum value in the Southern Ocean in (b) is about 0.04 W m^{-2}.

4. Results

a. With the resting ocean approximation

Figures 3a,b show the average rate of power input to the surface geostrophic currents by the NCEP monthly and 6-hourly winds, respectively. The spatial pattern in both cases is very similar to that found in previous studies (Wunsch 1998; Hughes and Wilson 2008; Scott and Xu 2009; Roquet et al. 2011), with the majority of the wind power input entering in the Southern Ocean. However, regions of both positive and negative power input become more pronounced when the 6-hourly wind is used. This change in magnitude can be clearly seen in Fig. 3c, which shows the power input by the 6-hourly wind minus that by the monthly wind. Positive power input is strongly enhanced in the Southern Ocean, Gulf Stream, and Kuroshio Extension when the synoptic values are used. In Figs. 3a,c, most of the wind power input north of 30°N in the North Atlantic and North Pacific is seen owing to wind periods between 6 h and a month, instead of the monthly- or climatological-mean

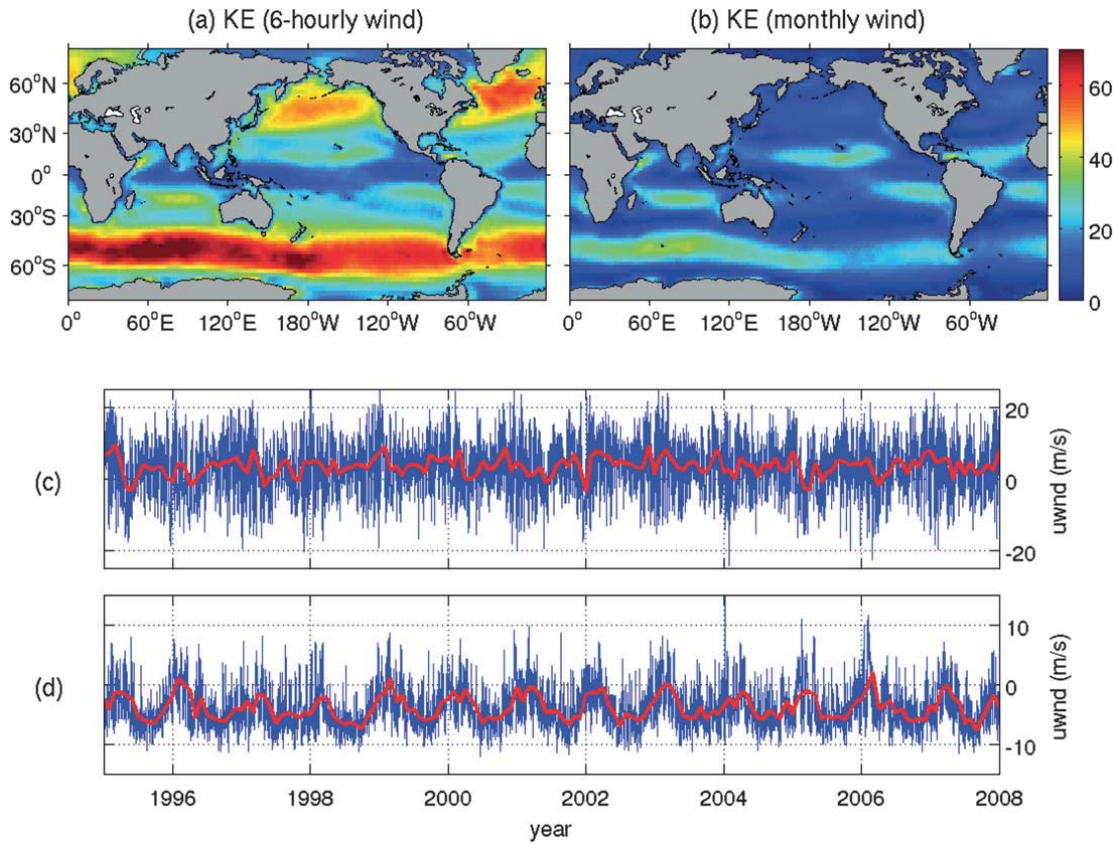

FIG. 4. The mean atmospheric kinetic energy ($\overline{|\mathbf{U}_{10}|^2}/2$; $m^2\ s^{-2}$) at 10 m above the sea surface computed using (a) the 6-hourly NCEP wind and (b) the monthly NCEP wind. The time series of the U component of 10-m winds at (c) (50°N, 326°E) and (d) (14°S, 185°E). The blue line represents the 6-hourly wind and the red line represents the monthly wind in (c) and (d).

values. The significant increase of wind power input to the surface geostrophic currents in the storm-track regions is consistent with the argument presented in section 2a because in these regions the synoptic wind variability is particularly strong. Figures 4a,b show the atmospheric kinetic energy $|\mathbf{U}_{10}|^2/2$ at 10 m above the sea surface associated with the 6-hourly and monthly NCEP winds, respectively. When averaged globally, the atmospheric kinetic energy associated with the 6-hourly wind is about 24 $m^2\ s^{-2}$, more than twice that associated with the monthly wind (about 10 $m^2\ s^{-2}$) and more than 3 times that associated with the time-mean wind (about 7 $m^2\ s^{-2}$). The monthly-mean wind represents a significant fraction of wind energy and variability at low latitudes, but the synoptic wind dominates over the monthly mean in the extratropical regions, especially in the storm-track regions. This geographic difference is further illustrated in Figs. 4c,d, which show the time series of 10-m winds at 50°N, 326°E in the storm-track region and 14°S, 185°E in the tropical region, respectively. The monthly-mean wind (red line) in the tropical South Pacific Ocean captures most of the wind variability there but fails completely at midlatitudes in the North Atlantic Ocean.

Integrated globally, the power input to the surface geostrophic currents by the monthly-mean wind is about 0.42 TW (1 TW = 10^{12} W), whereas that by the 6-hourly wind is about 0.72 TW (see Table 1), an increase of over 70%. The explanation for this significant increase in wind power input, as outlined in section 2, lies in the quadratic dependence of wind stress on wind itself, such

TABLE 1. The wind power input to the ocean general circulation by the monthly-mean NCEP wind stress taken directly from the reanalysis product and stresses computed from the 6-hourly, daily-mean, and monthly-mean NCEP 10-m winds. All numbers are globally integrated values in TW. In theory, estimates without the resting ocean approximation are more accurate. The most trustable estimates are highlighted in bold.

	Power input without the resting ocean approximation	Power input with the resting ocean approximation
Monthly NCEP wind	0.28	0.42
Daily NCEP wind	**0.42**	0.65
6-hourly NCEP wind	**0.47**	0.72
Monthly NCEP wind stress		0.87

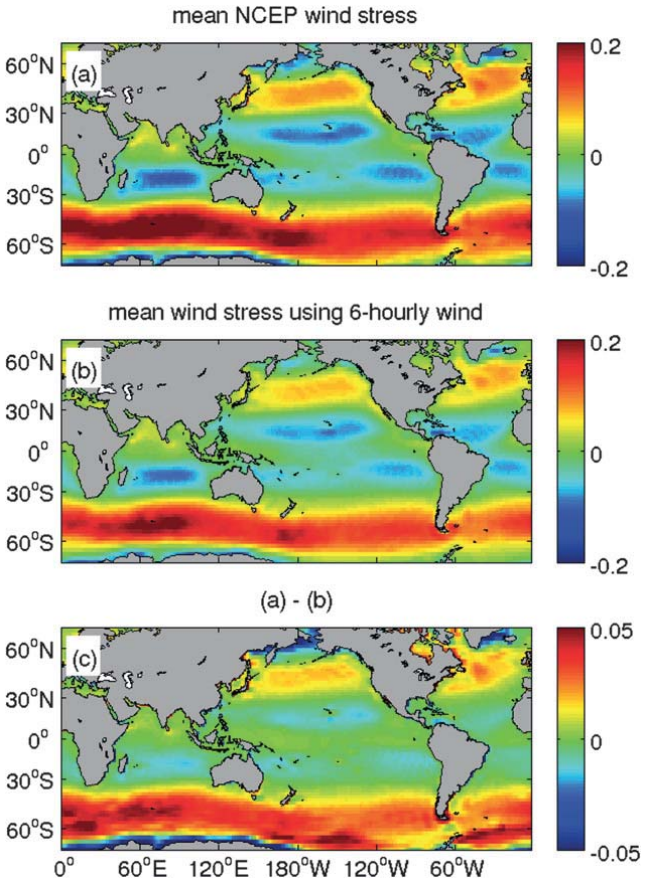

FIG. 5. The time-mean wind stress (N m^{-2}) by averaging (a) the monthly-mean NCEP wind stress taken directly from the reanalysis product and (b) the stress computed from the 6-hourly NCEP wind using (1) with $\mathbf{u}_o = 0$. (c) Shown is (a) minus (b).

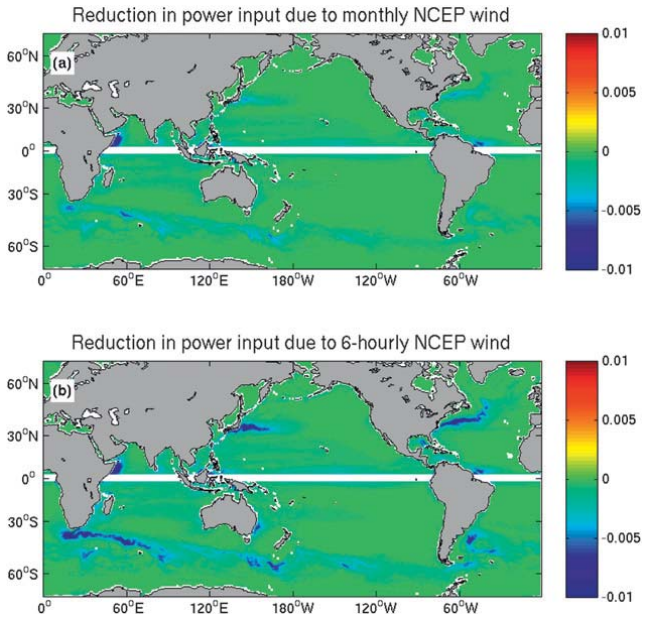

FIG. 6. The reduction in power input (W m^{-2}) associated with (a) the monthly NCEP wind and (b) the 6-hourly NCEP wind, after removing the resting ocean approximation. The color bar is as in Fig. 3 for easy comparison.

that the high-frequency wind contributes to the time-averaged wind stress. Wind power input to the ocean general circulation depends on the wind energy integrated over the whole spectrum. Power input by the daily wind integrates to about 0.65 TW, slightly less than that by the 6-hourly wind, and the difference is again concentrated in the storm-track regions (not shown). Readers are referred to Scott and Xu (2009) for an in-depth discussion of error estimates, where the authors found the uncertainty is about 10% of the mean using a range of wind and ocean current products.

It is possible that the time-dependent wind stress associated with the 6-hourly wind projects more effectively onto the time-dependent ocean surface velocities than does the stress associated with the monthly wind, and it could lead to an increase in wind power input. This possibility was tested by calculating the projection of time-dependent winds onto time-dependent currents, but no significant effect was found (see appendix B for a detailed discussion).

Figure 5 shows the time-mean wind stress by averaging the monthly NCEP wind stress taken directly from the reanalysis product, the time-mean wind stress computed from the 6-hourly wind using (1), and the difference between them. Note again that the monthly NCEP wind stress is a monthly average of the instantaneous surface wind stress at every 20-min NCEP model time step, and it therefore includes contributions from wind variability at all periods longer than 40 min. As a result, the wind stress computed using the 6-hourly wind still underestimates the NCEP modeled wind stress (Fig. 5c). This difference explains why the present estimate of wind power input to the ocean general circulation using the 6-hourly wind is somewhat less than previous estimates of ~0.9 TW when the resting ocean approximation is used (Wunsch 1998; Hughes and Wilson 2008; Scott and Xu 2009). Indeed, when the wind power input is computed directly using the monthly-mean NCEP wind stress, a value of 0.87 TW is obtained, closer to previous estimates. We will discuss this issue further in section 5.

b. Without the resting ocean approximation

In section 2b, it is argued that the synoptically varying wind can significantly reduce the energy of the surface geostrophic currents through the direct wind damping effect when the resting ocean approximation is not used. Figure 6 shows the reduction in power input by the monthly and 6-hourly NCEP winds because of the mechanical damping effect illustrated in Fig. 1. The spatial pattern is, again, very similar to that found in previous studies (Hughes and Wilson 2008; Scott and Xu 2009).

When integrated globally, the reduction in power input by the 6-hourly wind is about 0.25 TW, almost double the reduction by the monthly wind (0.14 TW; see Table 1). Hughes and Wilson (2008) estimated the reduction in power input to be ~0.19 TW using a weekly-mean wind, which fits well with the values in Table 1. One may anticipate that the mechanical damping effect by the wind will be even greater if the wind output from every NCEP time step is used.

5. Discussion

The quadratic dependence of the stress law on the wind speed produces a qualitative change in the calculation of power input to the ocean when synoptic weather systems are present. This result also amplifies the process by which the wind field damps eddy motions when the ocean surface velocity is accounted for. By comparing calculations from the NCEP 6-hourly, daily-mean, and monthly-mean estimated winds, the following is found

- Power input to the ocean general circulation is increased by roughly 70% when 6-hourly winds are used instead of monthly winds.
- With the resting ocean approximation, the power increase is from 0.42 to 0.72 TW (an increase of 71%). Much of the increase occurs in the storm-track regions of the Southern Ocean, Gulf Stream, and Kuroshio Extension.
- Without the resting ocean approximation, the power increase is from 0.28 to 0.47 TW (an increase of 68%).

There are substantial uncertainties in each of these figures; although the exact results presented in our study will depend quantitatively on the data and method used, the general ideas are generic and, we believe, robust.

With the resting ocean approximation, the power input by the 6-hourly wind is found to be about 0.2 TW less than that by the monthly-mean NCEP wind stress, which can be explained by the contribution of wind with periods less than 6 h to the monthly NCEP wind stress. However, this 0.2-TW difference raises a serious question: is the wind variability at such high frequencies (less than a few hours) really important for inputting energy to the geostrophic ocean circulation, which eventually finds its way to feed the deep-ocean mixing? Or does it simply generate shear, mixing, and waves (e.g., near-inertial waves) in the surface layer, with the majority of its energy input being dissipated there?[1] If the latter is true, the wind power input to the ocean general circulation that is relevant to deep-ocean mixing may be less than previously thought (~0.5 TW instead of ~1 TW).

Pathways by which the energy input by wind working on the sea surface enters the interior ocean circulation remain the subject of considerable uncertainty, partly because of the complex turbulent structure of the near-surface boundary layer (e.g., von Storch et al. 2007). As Roquet et al. (2011) show, the assumption of Ekman layer physics implies that the energy is pumped into the interior, sometimes far from the region of surface working. The accuracy of the wind products remains obscure, and previous estimates of possible factor of two errors in the total power input as calculated by these methods are probably still appropriate.

Finally, forcing ocean-only models is problematic. If ocean models are forced directly by the NCEP wind stress, they will be forced too strongly since the ocean surface velocity is not accounted for in the wind stress calculation. On the other hand, if ocean models are forced by the 6-hourly wind using (1), the energy input by the higher-frequency wind will be missed. Neither of these two caveats are trivial. Our study points toward the importance of coupled atmosphere–ocean models.

Acknowledgments. XZ thanks Benjamin Grandey and Chris Wilson for helpful discussions. Financial support was provided by the U.K. Natural Environment Research Council. HLJ is funded by a Royal Society University Research Fellowship, for which she is grateful. CW was supported by the George Eastman Visiting Professorship of Balliol College, Oxford. DPM is partially supported by the Oxford Martin School. We thank two anonymous reviewers for their constructive and insightful comments that led to significant improvements.

APPENDIX A

Mean Wind Stress Formula with Stochastic Variability

a. With the resting ocean approximation

It is assumed that the 10-m wind can be written as

$$U_{10} = \overline{U}_{10}(1 + \alpha z_t), \tag{A1}$$

where $\overline{U}_{10}$ is the time-mean 10-m wind and z_t is a normally distributed white noise with zero mean and unit variance: that is, $z_t \sim \mathcal{N}(0, 1)$. The probability density function of z_t is given by

[1] To leading order, the geostrophic flow does not exchange energy with the internal gravity wave field (Dewar and Killworth 1995).

$$f(x) = \frac{1}{\sqrt{2\pi}} e^{-(x^2/2)}. \quad \text{(A2)}$$

Substituting (A1) into $\tau = \rho_a c_d U_{10}^2$, we get

$$\tau = \rho_a c_d \overline{U}_{10}^2 (1 + \alpha z_t)^2 [2\mathcal{H}(1 + \alpha z_t) - 1], \quad \text{(A3)}$$

where $\mathcal{H}$ is the Heaviside step function. The time-averaged wind stress is then

$$\overline{\tau} = \rho_a c_d \overline{U}_{10}^2 \left[2 \int_{-1/\alpha}^{\infty} (1 + \alpha z_t)^2 \frac{e^{-z_t^2/2}}{\sqrt{2\pi}} dz_t - (1 + \alpha^2) \right]$$

and (A4)

$$= \rho_a c_d \overline{U}_{10}^2 \left[(1 + \alpha^2) \operatorname{erf}\left(\frac{1}{\sqrt{2}\alpha} \right) + \sqrt{\frac{2}{\pi}} \alpha e^{-(1/2\alpha^2)} \right], \quad \text{(A5)}$$

where erf() is the error function. The limits quoted in (5) follow through Taylor expansions and noting $2\sqrt{2/\pi} \approx 1.6$.

b. *Without the resting ocean approximation*

One can additionally include stochastic variability in the ocean currents as follows: We write the 10-m wind and ocean current speed as

$$U_{10} = \overline{U}_{10}(1 + \alpha \tilde{z}_t), \quad u_o = \gamma \overline{U}_{10}(1 + \beta \hat{z}_t),$$

where $\gamma \ll 1$ is a nondimensional parameter measuring the relative magnitudes of the wind and ocean current speeds and $\tilde{z}_t$ and $\hat{z}_t$ are uncorrelated white noises. It follows that

$$U_{10} - u_o = \overline{U}_{10}(1 - \gamma)(1 + \alpha^* \tilde{z}_t), \quad \text{(A6)}$$

where

$$\alpha^* = \frac{\sqrt{\alpha^2 + (\gamma\beta)^2}}{1 - \gamma} \approx \alpha(1 + \gamma) + O(\gamma^2). \quad \text{(A7)}$$

Thus, the previous solution with the resting ocean approximation remains valid with U_{10} replaced by $U_{10}(1 - \gamma)$ and α replaced by α^*. It also follows that stochastic variations in ocean current speed do not affect the mean stress to leading order, provided that the above scalings remain valid.

In the limits of small and large α, we obtain

$$\overline{\tau}_{\mathrm{DS}} = \begin{cases} (1 + \alpha^2 - 2\gamma)\tau + O(\gamma^2) & \text{for } \alpha \ll 1, \\ 1.6\alpha(1 - \gamma)\tau + O(\gamma^2) & \text{for } \alpha \gg 1; \text{ and} \end{cases} \quad \text{(A8)}$$

$$\Delta\overline{\tau}_{\mathrm{DS}} = \begin{cases} -2\gamma\tau + O(\gamma^2) & \text{for } \alpha \ll 1, \\ -1.6\gamma\alpha\tau + O(\gamma^2) & \text{for } \alpha \gg 1. \end{cases} \quad \text{(A9)}$$

APPENDIX B

The Time-Dependent Wind Power Input

It is possible that the time-dependent wind stress associated with the 6-hourly wind projects more effectively onto the time-dependent ocean surface velocities than does the stress associated with the monthly wind, and it could lead to an increase in wind power input. This possibility is tested here by considering the time-dependent component of the power input: that is, $\overline{\boldsymbol{\tau}' \cdot \mathbf{u}_g'}$, where primes represent deviations from the 14-yr time average. Figure B1 shows this time-dependent power input associated with the monthly NCEP wind stress taken directly from the reanalysis product and wind stresses computed from the 6-hourly and monthly winds. The time-dependent wind power input at low latitudes, which has the most organized structure and dominates the total time-dependent wind power input, is very similar among the three wind products, consistent with the fact that the monthly wind dominates the wind power input there (Fig. 4). At middle and high latitudes, there are much more pronounced patches of positive and negative values in the storm-track regions in Figs. B1b,c, but they largely cancel out when integrated spatially. The time-dependent wind power input in the Indian Ocean, associated with the seasonally reversing monsoon wind, accounts for almost all the wind power input there for each wind product. Another interesting feature that shows up for all three wind products is a narrow band of positive time-dependent power input in the tropical North Pacific (and also in the tropical North Atlantic) underneath the intertropical convergence zone (ITCZ). Integrated globally, the time-dependent component of the power input is about 0.04 TW for the monthly wind and about 0.06 TW for the 6-hourly wind and monthly NCEP wind stress. Therefore, although the time-dependent wind stress associated with the 6-hourly wind does seem to project better onto the time-dependent ocean surface velocities than the stress associated with the monthly wind, it makes only a very small contribution toward the 0.3-TW increase of wind power input when the 6-hourly wind is used.

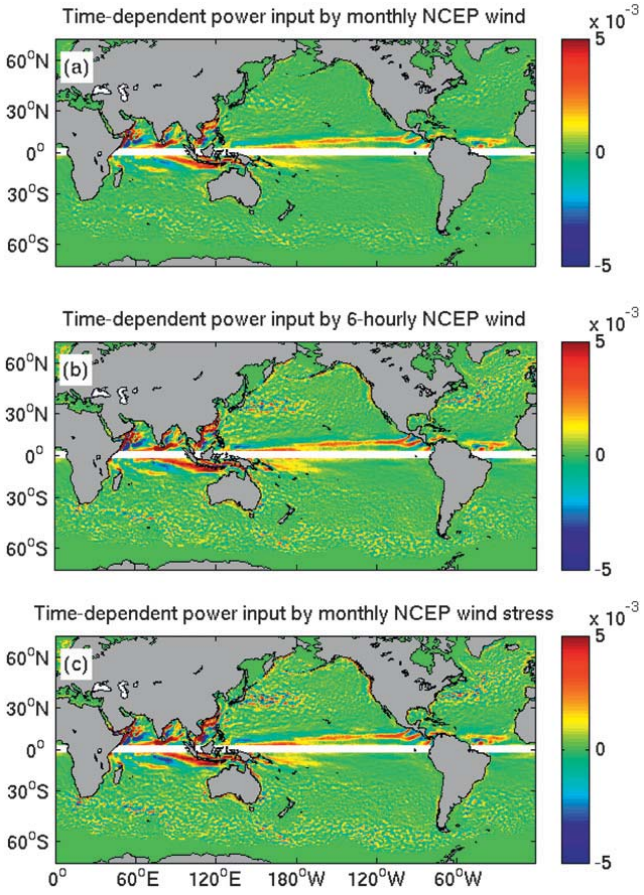

FIG. B1. The time-dependent component of the power input $\overline{\boldsymbol{\tau}' \cdot \mathbf{u}_g'}$ by (a) the stress computed from the monthly NCEP wind, (b) the stress computed from the 6-hourly NCEP wind, and (c) the monthly-mean NCEP wind stress taken directly from the reanalysis product. Note the different color scale from Fig. 3.

REFERENCES

Dewar, W. K., and P. D. Killworth, 1995: Do fast gravity waves interact with geostrophic motions? *Deep-Sea Res.,* **42,** 1063–1081.

Duhaut, T. H., and D. N. Straub, 2006: Wind stress dependence on ocean surface velocity: Implications for mechanical energy input to ocean circulation. *J. Phys. Oceanogr.,* **36,** 202–211.

Ferrari, R., and C. Wunsch, 2009: Ocean circulation kinetic energy: Reservoirs, sources, and sinks. *Annu. Rev. Fluid Mech.,* **41,** 253–282.

Hughes, C. W., and C. Wilson, 2008: Wind work on the geostrophic ocean circulation: An observational study on the effect of small scales in the wind stress. *J. Geophys. Res.,* **113,** doi:10.1029/2007JC004371.

Kalnay, E., and Coauthors, 1996: The NCEP/NCAR 40-Year Reanalysis Project. *Bull. Amer. Meteor. Soc.,* **77,** 437–471.

Large, W. G., J. C. McWilliams, and S. C. Doney, 1994: Oceanic vertical mixing: A review and a model with a nonlocal boundary layer parameterization. *Rev. Geophys.,* **32,** 363–403.

Le Traon, P. Y., F. Nadal, and N. Ducet, 1998: An improved mapping method of multisatellite altimeter record. *J. Atmos. Oceanic Technol.,* **15,** 522–534.

Maximenko, N. A., and P. P. Niiler, 2005: Hybrid decade-mean global sea level with mesoscale resolution. *Recent Advances in Marine Science and Technology,* N. Saxena, Ed., PACON International, 55–59.

Roquet, F., C. Wunsch, and G. Madec, 2011: On the patterns of wind-power input to the ocean circulation. *J. Phys. Oceanogr.,* **41,** 2328–2342.

Scott, R. B., and Y. Xu, 2009: An update on the wind power input to the surface geostrophic flow of the World Ocean. *Deep-Sea Res.,* **56,** 295–304.

Thompson, K. R., R. F. Marsden, and D. G. Wright, 1983: Estimation of low-frequency wind stress fluctuations over the open ocean. *J. Phys. Oceanogr.,* **13,** 1003–1011.

von Storch, J. S., H. Sasaki, and J. Marotzke, 2007: Wind-generated power input to the deep ocean: An estimate using a 1/10 general circulation model. *J. Phys. Oceanogr.,* **37,** 657–672.

Wunsch, C., 1998: The work done by the wind on the oceanic general circulation. *J. Phys. Oceanogr.,* **28,** 2332–2340.

Zhai, X., and R. J. Greatbatch, 2007: Wind work in a model of the northwest Atlantic Ocean. *Geophys. Res. Lett.,* **34,** L04606, doi:10.1029/2006GL028907.

——, ——, C. Eden, and T. Hibiya, 2009: On the loss of wind-induced near-inertial energy to turbulent mixing in the upper ocean. *J. Phys. Oceanogr.,* **39,** 3040–3045.